

3-D Numerical Modeling of Heat Transport Phenomena in Soil under Climatic Conditions of Southern Thailand

Jompob WAEWSAK^{1,*}, Narit KLOMPONG¹ and Kornvika KONGKUL²

¹*Solar and Wind Energy Research Laboratory (SWERL), Research Center in Energy and Environment, Department of Physics, Faculty of Science, Thaksin University, Phatthalung 93110, Thailand*

²*Department of Mathematics and Statistics, Faculty of Science, Thaksin University, Phatthalung 93110, Thailand*

(* Corresponding author's e-mail: jompob@tsu.ac.th)

Received: 29 December 2011, Revised: 8 December 2014, Accepted: 29 January 2015

Abstract

This paper presents a 3-D numerical modeling of heat transport phenomena in soil due to a change of sensible and latent heat, under the ambient conditions of southern Thailand. The vertical soil temperature profile within 3 m was predicted based on energy balance and 3 modes of heat transfer mechanisms, i.e., conduction, convection, and radiation. Mathematical models for estimation of solar radiation intensity, ambient and sky temperatures, relative humidity, and surface wind velocity were used as model inputs. 3-D numerical implicit finite difference schemes, i.e., forward time, and forward, center, and backward spaces were used for discretizing the set of governing, initial, and boundary condition equations. The set of pseudo-linear equations were then solved using the single step Gauss-Seidel iteration method. Computer code was developed by using MATLAB computer software. The soil physical effects; density, thermal conductivity, emissivity, absorptivity, and latent heat on amplitude of soil temperature variation were investigated. Numerical results were validated in comparison to the experimental results. It was found that 3-D numerical modeling could predict the soil temperature to almost the same degree as results that were obtained by experimentation, especially at a depth of 1 m. The root mean square error at ground surface and at depths of 0.5, 1, 1.5, 2, 2.5 and 3 m were 0.169, 0.153, 0.097, 0.116, 0.120, 0.115, and 0.098, respectively. Furthermore, it was found that variation of soil temperature occurred within 0.75 m only.

Keywords: Finite difference, heat transfer, numerical modeling, soil

Introduction

Soil temperature is one of the most important parameters in applications of passive heating and cooling of buildings, and in engineering systems, such as ground heat storage, heat pump ground heat exchangers, and agricultural greenhouses. Many applications, e.g. direct and indirect contact with the soil of either building envelopes or greenhouses, which involve the use of buried pipes [1-3], require knowledge of the underground temperature distribution. The underground temperature distribution is affected by the structure and physical properties of the soil, ground surface cover, e.g. bare ground and lawn, and climatic interaction, determined by solar radiation, air temperature, wind, air humidity, and rainfall. The ground zone can be distinguished into the surface zone (1 m), in which the ground temperature is very sensitive to short time changes of weather conditions; the shallow zone, which extends from a depth of about 1 - 8 m, where the ground temperature is almost constant and close to the annual air temperature; and the deep zone (below about 8 - 20 m), which is the zone where the ground temperature is practically constant, and very slowly rises with depth, according to the geothermal gradient [4]. Many research works have shown that soil temperatures at shallow depths present significant

fluctuations on both a daily and annual basis, going against the belief that the soil temperature distribution at any depth below the earth's surface is unchanged throughout the year [5,6]. The thermal properties of soil are also required in many areas of soil science, agronomy, and engineering. The thermal conductivity of a soil depends on several factors, such as the texture and mineralogical composition of the soil. However, there are 2 main factors influencing the thermal conductivity of a soil, i.e., water content and soil bulk density [7]. The water content of the soil affects its temperature pattern. The thermal conductivity and volumetric heat capacity increase with the water content of the soil and determines the heat transfer rate inside the soil. Since moisture content can change with time and depth, these bulk properties may also vary, complicating attempts at soil temperature estimation. The soil can gain or lose heat in its interaction with water at different temperatures, and absorbs or dissipates heat during phase change, i.e., evaporation, condensation, freezing, melting, or sublimation. The most important of these processes is evaporation, although, in dry zones, evaporation plays a much smaller part in the surface energy balance [8]. Nevertheless, a simple methodology, that deals with the application of an insertion tensiometer to estimate the moisture migration in the soil mass due to thermal gradient, has been developed and presented [9], and the relationship between ground temperature and the air relative humidity, as well as evaporation, has also been presented [10].

In Thailand, measurements of soil temperature at 0.05, 0.1, 0.2, 0.5, and 1 m are routinely accomplished by the Thai Meteorological Department at various agro-meteorological stations installed spread throughout the Kingdom of Thailand, and the data are analyzed and reported on an annual report basis. The measurements of soil temperature at surface and various depths are spatial and temporal limited. It requires a lot of apparatus; thus, the experimentation execution necessitates a high cost. A variety of mathematical models for the prediction of the soil temperature as a function of depth, season, and soil properties, based on analysis of multiyear measurements or on Fourier analysis, have already been developed and presented [11-13]. Unfortunately, a model based upon the energy balance and heat loss due to evaporation for the prediction of soil temperature at various depths under the climatic conditions of southern Thailand has never been carried out. Consequently, this paper aims at presenting 3-D numerical modeling for predicting soil temperature in order to investigate the vertical soil temperature profile and temporal variation. For the sake of simplicity, all energy balance equations are taken into consideration in the model, except for water content. The energy balance equations involve energy exchange between air and soil, the solar radiation absorbed by the soil surface, heat convection by surface wind, and long-wave radiation to the sky. Furthermore, the heat loss due to the evaporation process was also included in the model. The model was validated using extensive sets of measurements for bare and short-grass soil in the Phatthalung province of southern Thailand.

Materials and methods

Assumptions

For simplicity and validity of the model, the following assumptions were made:

- (1) Soil is considered as a homogeneous material.
- (2) The physical properties of soil are temperature independent.
- (3) The downward atmospheric radiation originated under clear sky can be considered as gray body radiation.

With these important assumptions, the heat transport phenomena in soil could be considered and analyzed, using nodal heat transfer mechanism and finite difference numerical methods.

Heat transport phenomena in soil

Heat transport phenomena in soil are natural processes under environmental conditions, consisting of 3 main mechanisms of heat transfer, i.e., conduction, convection, and radiation, which cause change in soil temperature. Based on energy balance, some heat was lost due to the evaporation process. Water content will affect this process, since it depends on the concentration of moisture in soil or the condition of saturation. During the day, soil absorbs solar radiation. The amount of heat absorbed depends on the heat capacity of soil. Heat loss is due to convection to ambient air and long-wave radiation to the cooler

sky. Heat is transferred by conduction to the deeper soil and by the latent heat of evaporation in soil due to moisture content. The process heat transfer during the day is shown in **Figure 1**. On the other hand, during the night, heat transfer phenomena will reverse, due to there being no solar radiation and the cooler night sky. The absorbed heat in soil during the day will transfer to the cooler heat sink, i.e., ambient air and night sky by convection and long-wave radiation, respectively. Partly, heat is transferred by the evaporation process in soil. The heat transport phenomena during the night are shown in **Figure 2**.

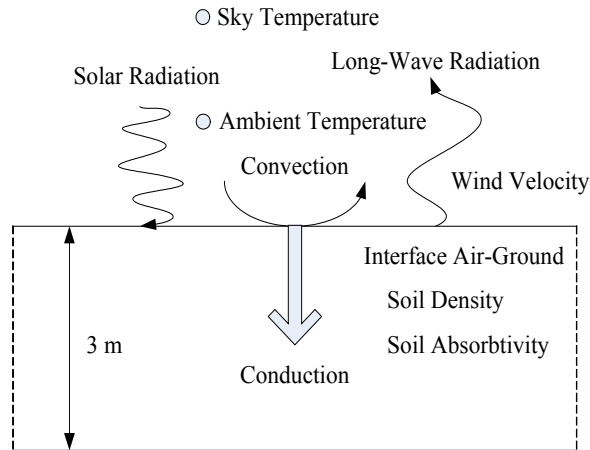


Figure 1 Diurnal soil heat transport phenomenon.

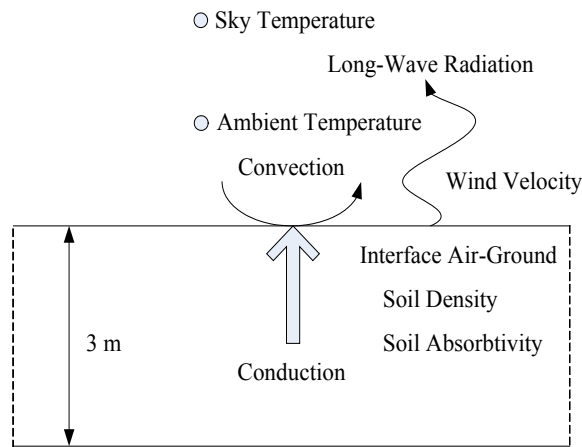


Figure 2 Nocturnal soil heat transport phenomenon.

Governing equations

The governing equations are set based upon the partial derivative equations (PDEs) of heat diffusion equations in soil, which are parabolic equations as given in Eqs. (1) and (2) [14].

$$c_p \rho \frac{\partial T}{\partial t} = k \left(\frac{\partial^2 T}{\partial x^2} + \frac{\partial^2 T}{\partial y^2} + \frac{\partial^2 T}{\partial z^2} \right) \quad (1)$$

$$\frac{\partial T}{\partial t} = D \left(\frac{\partial^2 T}{\partial x^2} + \frac{\partial^2 T}{\partial y^2} + \frac{\partial^2 T}{\partial z^2} \right) \quad (2)$$

where T is the temperature (K), ρ is the soil density, c_p is the heat capacity of soil, t is the time, k is the thermal conductivity, D is the thermal diffusivity, and x - y - z is the direction in the x -axis, y -axis, and z -axis, respectively.

Input parameters

The input parameters consist of climatological conditions, i.e., global solar radiation intensity, ambient temperature, sky temperature, wind velocity, and relative humidity. They were generated using the developed mathematical models from many researchers, i.e., hourly global solar radiation intensity, hourly ambient, and sky temperatures [15-19]. Hourly wind velocity and relative humidity in Phatthalung province were modeled using the meteorological data collected during 1990 - 2000 [20].

Global solar radiation is the most important input parameter affecting soil temperature variation. It was modeled using the well known Angstrom's equation [15]. Although this model was developed to predict global solar radiation in 1994, it is still valid, due to the there being little change in global solar radiation. The variation of global solar radiation in Phatthalung province on 4 typical major dates is shown in **Figure 3**.

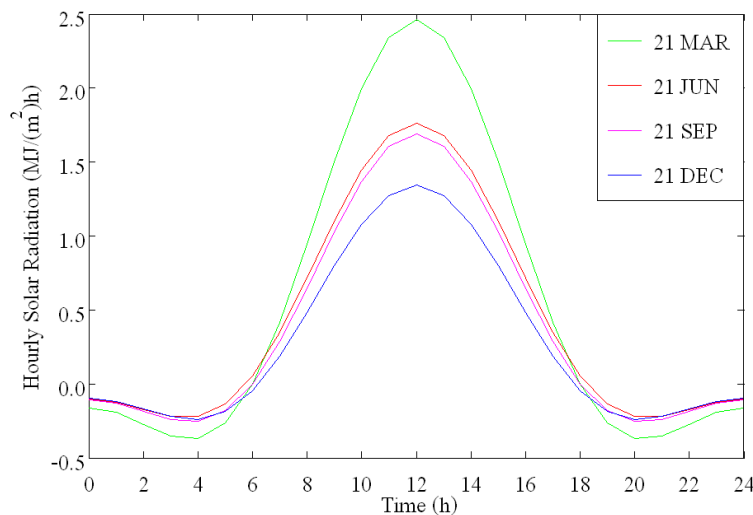


Figure 3 Variation of global solar radiation in Phatthalung province on 4 typical major dates.

The variation of wind velocity, ambient temperature, and sky temperature is shown in **Figures 4 - 6**, respectively. The variation of hourly percent relative humidity is applied using the model developed based on the observed data collected in 1995 - 2005, as shown in **Figure 7** [21].

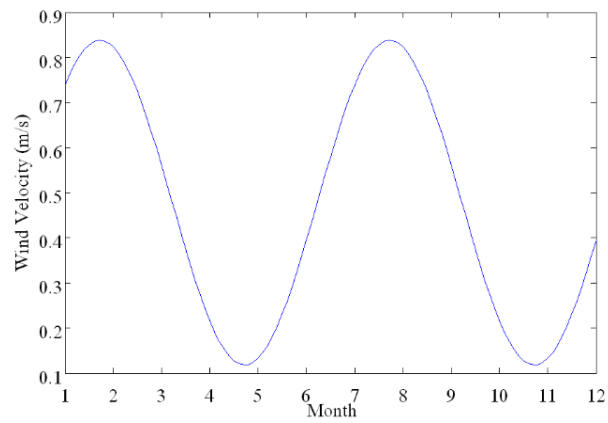


Figure 4 Hourly wind velocity in Phatthalung province.

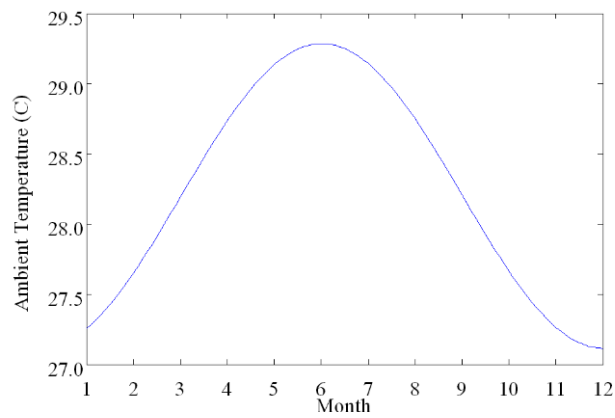


Figure 5 Monthly ambient temperature in Phatthalung province.

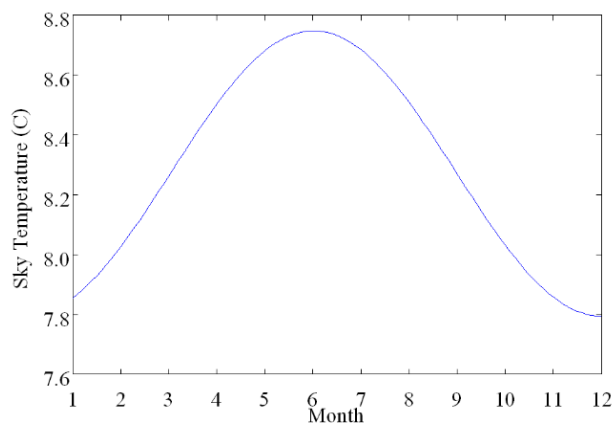


Figure 6 Monthly sky temperature in Phatthalung province.

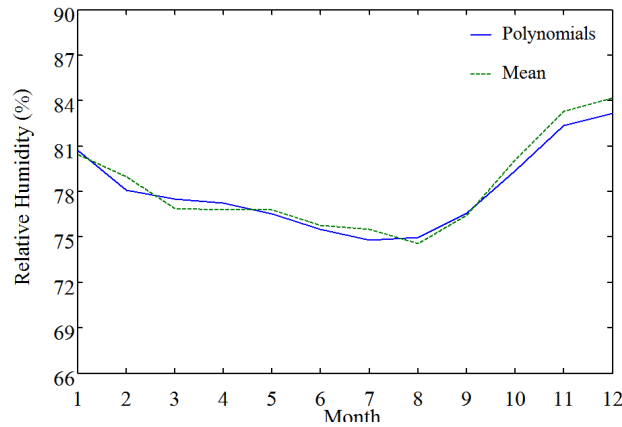


Figure 7 Monthly percent relative humidity in Phatthalung province.

Initial and boundary conditions

(1) Initial conditions

The initial conditions were used in the single step Gauss-Seidel iteration method. For numerical solution, the temperature at any given node was kept at $T_{i,j,k} = 27\text{ }^{\circ}\text{C}$. The symbol i, j and k represents x -axis, y -axis, and z -axis, respectively.

(2) Boundary conditions

A control volume of soil, which had 6 boundaries, i.e., a top, 4 sideways, and a bottom, were considered as boundary conditions. For the top boundary, or the surface of soil, there are many interactions between the soil and the surrounding environment, including the absorption of solar radiation and heat loss from soil due to evaporation, long-wave radiation to the sky, heat conduction to the deeper zone, and convection by ambient air. However, as the change of boundary condition depends on time, it means that the diurnal boundary condition and the nocturnal boundary condition will determine the soil heat transfer direction. During daytime, heat will transfer downward. On the other hand, during the night, heat will transfer upward. The change in heat transfer direction occurs on a daily basis. Based upon the energy balance and heat transfer phenomenon during the day and the night, the boundary condition of soil surface nodes, as illustrated in **Figure 8**, can be obtained in Eqs. (3) - (4).

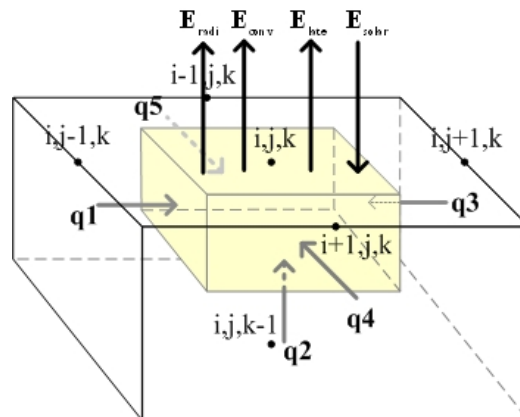


Figure 8 Boundary conditions at surface (i, j , and k represents x -axis, y -axis, and z -axis).

$$E_{st} = E_{solar} - E_{conv} - E_{late} - E_{radi} - E_{cond} \tag{3}$$

$$\rho c_p A \frac{\Delta z \Delta T}{2 \Delta t} = \frac{A \alpha I}{3600} - h_c A (T_{i,j,k}^{p+1} - T_a) - h_r A (T_{i,j,k}^{p+1} - T_s) - F(u) [b(1 - Rh) - a(Rh T_a - T_{sur})] + q1 + q2 + q3 + q4 + q5 \tag{4}$$

where α is the absorption coefficient, I is the solar radiation intensity, $q1$, $q3$, $q4$ and $q5$ is the heat transfer from the sideward, $q2$ is the heat transfer from the bottom, A is the area of heat transfer, Δx , Δy , and Δz are the gap spacing, Δt is the time increment, h_c and h_r are the convective and radiative heat transfer coefficients, $F(u)$ is the latent heat of evaporation, Rh is the relative humidity, a and b are the constants, and subscripts a , sur and s mean air, surrounding, and soil, respectively.

Figure 9 shows the boundary conditions of sideward nodes. The boundary conditions obtained by the energy balance, i.e., input energy equal to output energy, are given in Eqs. (5) - (6). The boundary conditions of the bottom nodes are given in Eq. (7).

$$T_{1,j,k}^p = (1 + 6Fo) T_{1,j,k}^{p+1} - Fo (2T_{2,j,k}^{p+1} + T_{1,j+1,k}^{p+1} + T_{1,j-1,k}^{p+1} + T_{1,j,k+1}^{p+1} + T_{1,j,k-1}^{p+1}) \tag{5}$$

where $i = 1$ $j = 2, 3, 4 \dots n-1$ and $k = 2, 3, 4 \dots n-1$.

$$T_{n,j,k}^p = (1 + 6Fo) T_{n,j,k}^{p+1} - Fo (2T_{n-1,j,k}^{p+1} + T_{n,j+1,k}^{p+1} + T_{n,j-1,k}^{p+1} + T_{n,j,k+1}^{p+1} + T_{n,j,k-1}^{p+1}) \tag{6}$$

where $i = n$ $j = 2, 3, 4 \dots n-1$ and $k = 2, 3, 4 \dots n-1$.

$$T_{i,j,n}^p = (1 + 6Fo) T_{i,j,n}^{p+1} - Fo (T_{i+1,j,n}^{p+1} + T_{i-1,j,n}^{p+1} + T_{i,j+1,n}^{p+1} + T_{i,j-1,n}^{p+1} + 2T_{i,j,n-1}^{p+1}) \tag{7}$$

where $i = 2, 3, 4 \dots n-1$ $j = 2, 3, 4 \dots n-1$ and $k = n$.

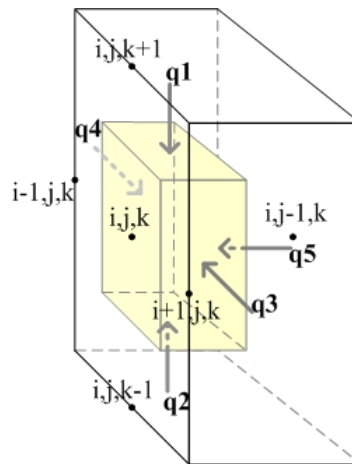


Figure 9 Boundary conditions at sideward nodes (i , j , and k represents for x -axis, y -axis, and z -axis).

Numerical technique

The sets of governing equations and boundary conditions were discretized using the implicit scheme, as well as the Forward Time Centered Space (FTCS) scheme for interior nodes, the Forward Time Backward Space scheme for the deepest node, and the Forward Time Forward Space scheme for the node at the surface, as shown in Eq. (8);

$$T_{i,j,k}^p = (1 + 6Fo)T_{i,j,k}^{p+1} - Fo(T_{i+1,j,k}^{p+1} + T_{i-1,j,k}^{p+1} + T_{i,j+1,k}^{p+1} + T_{i,j-1,k}^{p+1} + T_{i,j,k+1}^{p+1} + T_{i,j,k-1}^{p+1}) \quad (8)$$

where Fo is the Fourier number [20].

The sets of linearized equations were rearranged to form the augmented matrix. The single step Gauss-Seidel iteration with initial values was used for solving the set of equations. The grid spacing in the x-y-z direction was 0.25 m, and the time increment was 900 s. The set of 2,197 equations were solved simultaneously. The computation was stopped, as the error met the stopping criteria (≤ 0.01). The flowchart for computation is shown in **Figure 10**.

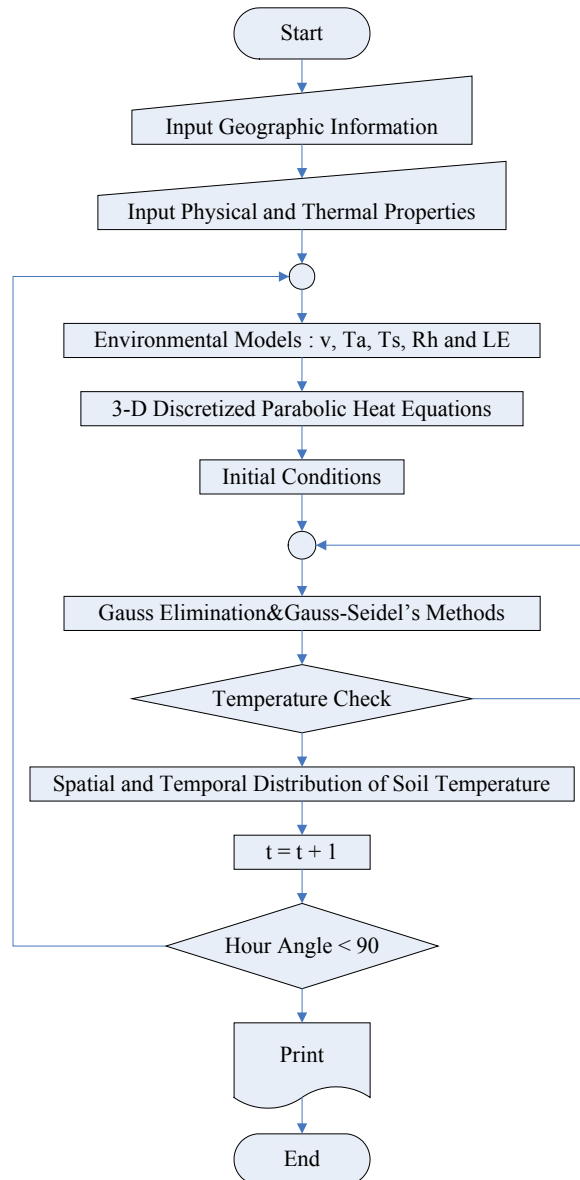


Figure 10 Flowchart for computation.

Model validation

A field measurement was set up in order to measure the soil temperature profile in Phatthalung province in 2007, as shown in **Figure 11**. It was conducted in the field in Thaksin University (Phatthalung Campus). Experimentation was carried out in order to collect the experimental data for validation of the numerical results. The temperature of soil at depths of 0.5, 1.0, 1.5, 2.0, 2.5, and 3.0 m was measured using the type “K” sheath thermocouple, connected to a memory data logger model: HIOKI 842 1-51 Serial No: 5073687 3. The soil moisture content was also measured at depths of 1.0, 1.5, and 2.0 m, using the EE-04 soil moisture sensors. The variation of the ambient temperature and humidity, wind speed and direction, and the intensity of solar radiation were measured using a humidity and temperature transmitter model: TRH-303, a wind speed and direction sensor, and a pyranometer model: ML - 020 VM, respectively. All parameters were transmitted via a transmitter and resistance model: TR-9IB, except the direction signal via a transmitter and frequency model: TMF-3IB. The UPS for 500 VAC 220 V was used for a power supply at the field testing. The validation was executed using the root mean square error (RMSE), in order to perform the model performance.

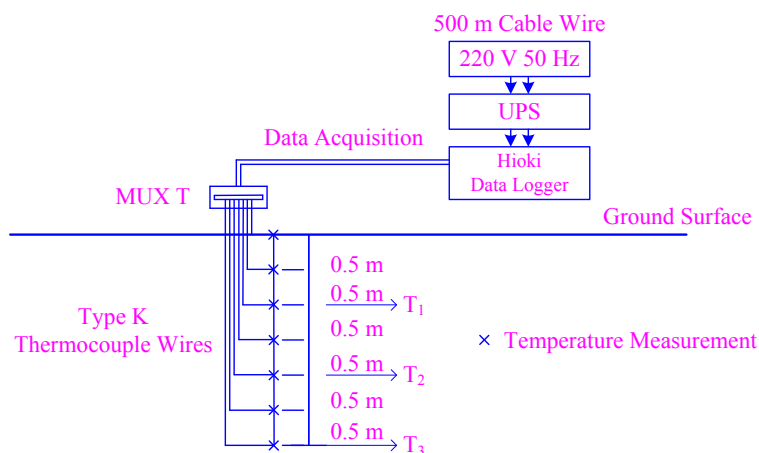


Figure 11 Experimental set up for soil temperature measurement.

Results and discussion

The temporal variation of soil temperature was investigated based on the numerical modeling. The effect of density, thermal conductivity, emissivity, absorptivity, and latent heat were investigated and are presented in this paper. The RMSE was analyzed in order to validate the numerical results with the experimental results performed under the real conditions of Phatthalung province in southern Thailand.

Soil temperature variation

Numerical results showed that the spatial variation of soil temperature, especially in the x and y directions, were the same, as shown in **Figures 12 – 13**, while the variation of soil temperature in the z-direction occurred near the soil surface within 0.75 m only, as shown in **Figure 14**. Beyond 0.75 m, the soil temperature was constant.

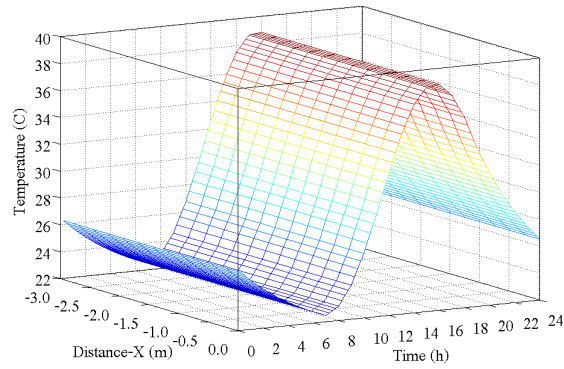


Figure 12 Variation of soil temperature along the x-axis (horizontal plane of soil).

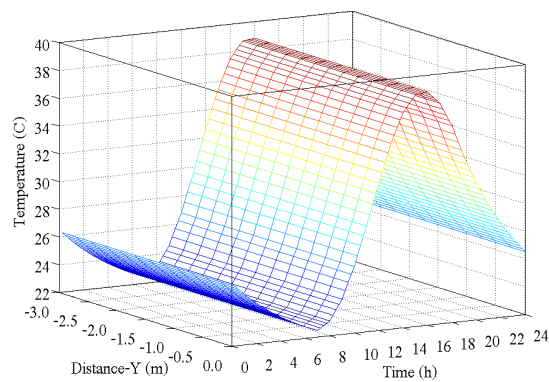


Figure 13 Variation of soil temperature along the y-axis (horizontal plane of soil).

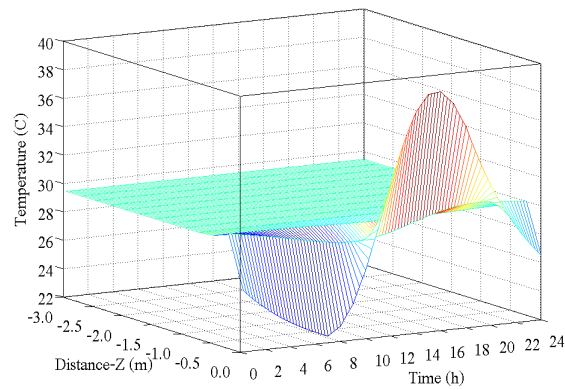


Figure 14 Variation of soil temperature along the z-axis (soil depth).

Figure 15 clearly shows that the variation of soil temperature occurred at the soil surface (node 1), while the soil temperature of node 2 was varied slightly.

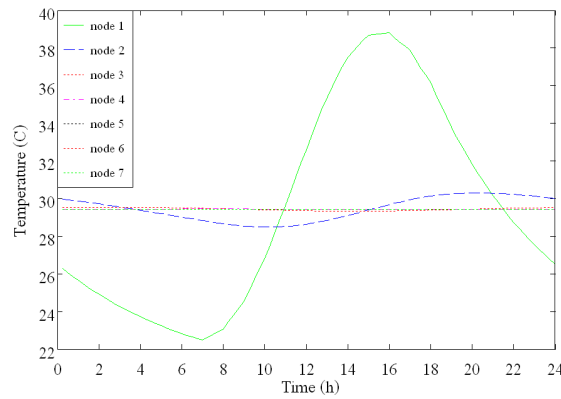


Figure 15 Temporal variation of soil temperature near the surface (delta x = 0.25 m).

Effect of soil density

Figure 16 shows the effect of soil density on the variation of soil temperature. The soil density varied in the range of 1,000 - 2,000 kg/m³, with 250 kg/m³ intervals. It was found that the surface soil temperature decreased while the soil density increased. This was due to the increasing of soil density, which enhanced the heat transfer rate. The heat conduction mechanism requires media for heat transfer; therefore, the higher the soil density, the more the heat transfer rate. The vertical profile of soil temperature at various soil densities is shown in Figure 17.

It can be seen that the effect of soil density plays a major role within 0.75 m. At depths over 0.75 m, the soil density did not play any significant effect. However, it is interesting to know that, the lower the soil density, the higher the difference of soil temperature, between the surface and 0.25 m.

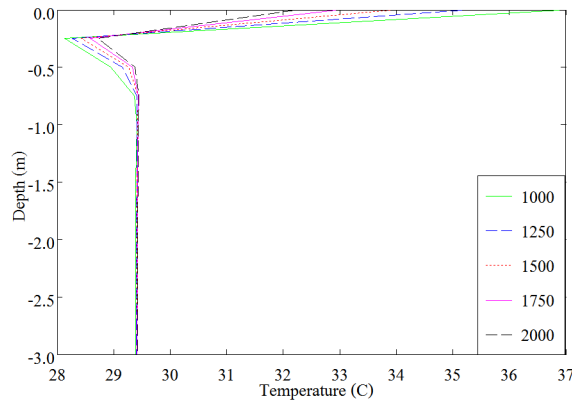


Figure 16 Time-dependent variation of surface soil temperature at various soil densities.

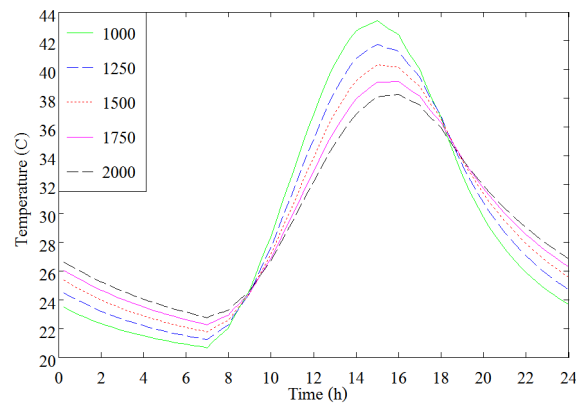


Figure 17 Vertical profile of soil temperature at various soil densities.

Effect of thermal conductivity

It is obvious that the higher soil thermal conductivity, the lower the soil temperature, as shown in **Figure 18**. The thermal conductivity of soil does affect the amplitude of soil temperature variation. The highest peak of soil temperature occurred with the lowest soil thermal conductivity.

Furthermore, the positive peak of soil temperature occurred at 3 p.m., while the negative peak occurred at 7 a.m. However, the thermal conductivity did not affect the vertical profile of soil temperature, as can be observed in **Figure 19**.

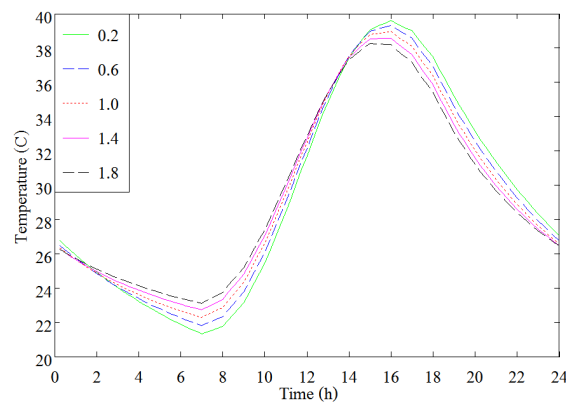


Figure 18 Time-dependent variation of soil temperature at various thermal conductivities.

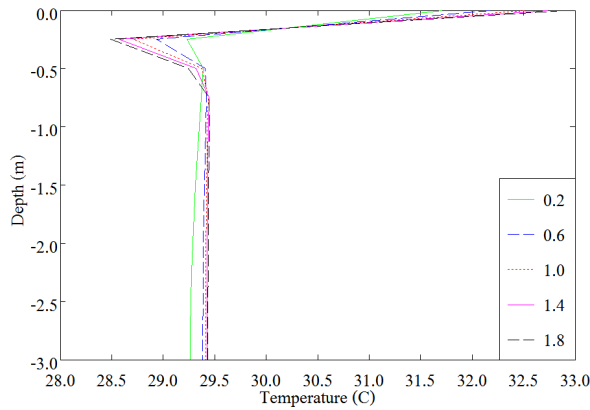


Figure 19 Vertical profile of soil temperature at various thermal conductivities.

Effect of soil emissivity

The emissivity of soil plays a major role in variation of soil temperature, since the emissivity of soil varied in the range of 0.35 - 0.95. The gradient of soil temperature variation occurred largely as shown in **Figure 20**. It can be found, from **Figure 20**, that the lower the soil emissivity, the higher the soil temperature.

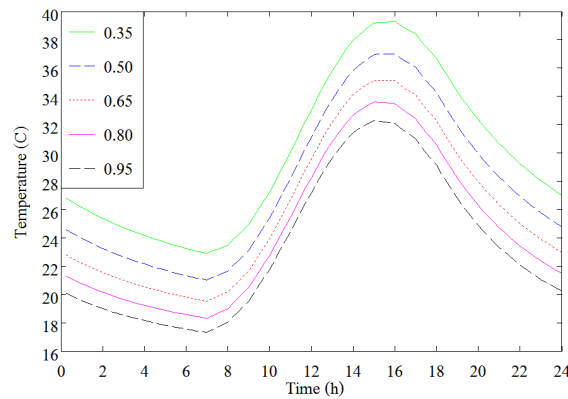


Figure 20 Time-dependence of soil temperature at various soil emissivities.

Figure 21 also shows the effect of soil emissivity on vertical temperature profile. The soil emissivity difference in the range of 0.55 caused the soil temperature difference in the range of 7 °C.

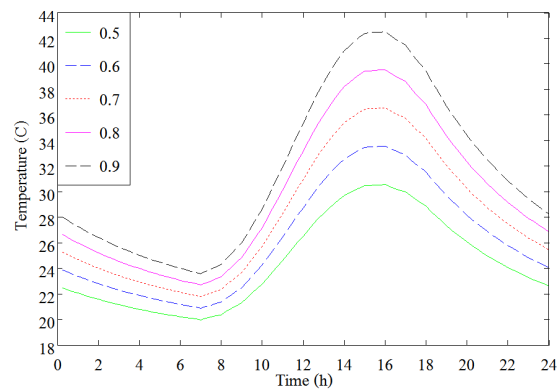


Figure 21 Vertical profile of soil temperature at various emissivities.

Effect of soil absorptivity

In contrast to the effect of emissivity, the soil absorptivity plays a significant role on soil surface energy input, especially the absorption of incident solar radiation. The soil absorptivity depends upon the cover of soil surface, e.g., bare, lawn, and vegetable covers. The higher the soil absorptivity, the more the soil temperature, as shown in **Figure 22**. The soil absorptivity variance in the range of 0.5 - 0.9 caused the temperature difference of 7 °C, as displayed in **Figure 23**.

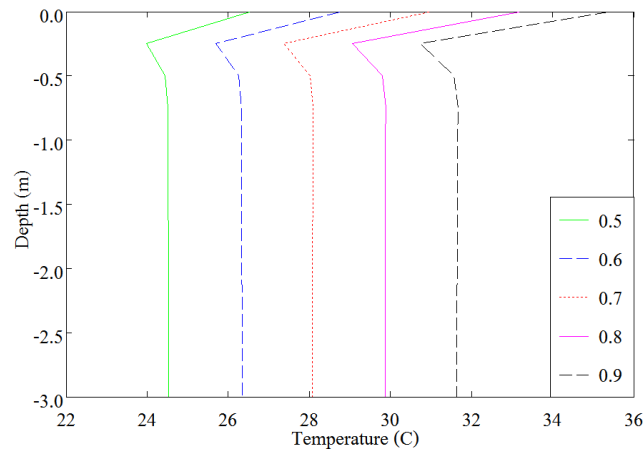


Figure 22 Time-dependence of soil temperature at various absorptivities.

Effect of latent heat

Latent heat has a much more significant effect when compared to any other physical parameters of soil.

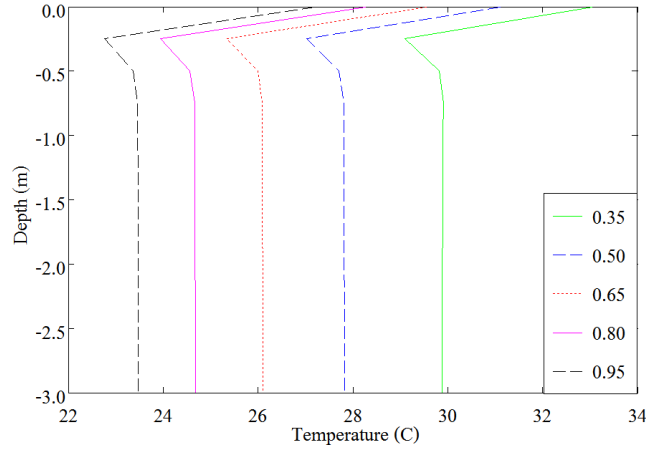


Figure 23 Vertical profile of soil temperature at various absorptivities.

Since the factor for latent heat change varies from 0 - 1, with 0.25 intervals, this means that the phase change of water in soil either does or does not occur. The number assigned to heat extracted from the soil was high when the latent heat changed from 0 to 0.25 as the soil temperature decreased, as shown in **Figure 24**. It can be seen that if the factor for latent heat continued to increase, the soil temperature decreased towards a negative value. This means that most of the heat in soil was extracted to evaporate the moisture in soil. But in reality, the soil temperature in Thailand is never below 15°C; therefore, the factor for latent heat should not exceed 0.25. The vertical soil temperature profile due to effect of latent heat is shown in **Figure 25**.

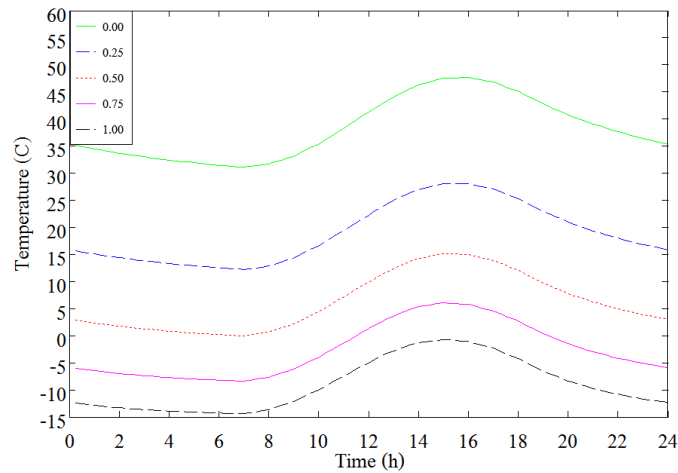


Figure 24 Time-dependence of soil temperature at various latent heats.

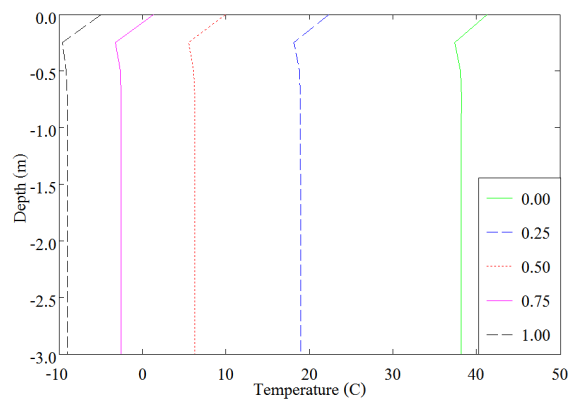


Figure 25 Vertical profile of soil temperature at various latent heats.

Model validation

It was found that the RMSE was in the range of 0.097 - 0.169, as shown in **Table 1**. Furthermore, the minimum RMSE was found to be 0.097 at a depth of 1.0 m, whereas the maximum RMSE was found to be 0.169 at the soil surface. The comparison of predicted and observed hourly soil temperature at various depths is shown in **Figure 26**. This means that the measured data and the predicted data were almost the same. Therefore, it can be claimed that the 3-D transient numerical simulation of soil temperature under the implicit finite difference scheme was valid, and can be used for prediction of soil temperature at different locations in Thailand when the input data are known. Nevertheless, the model accuracy could be increased by applying mass transfer phenomena into the model. This should be a further step in development of this kind of modeling.

Table 1 RMSE at various depths.

Depth (m)	RMSE
0.0	0.169
0.5	0.153
1.0	0.097
1.5	0.116
2.0	0.120
2.5	0.125
3.0	0.098

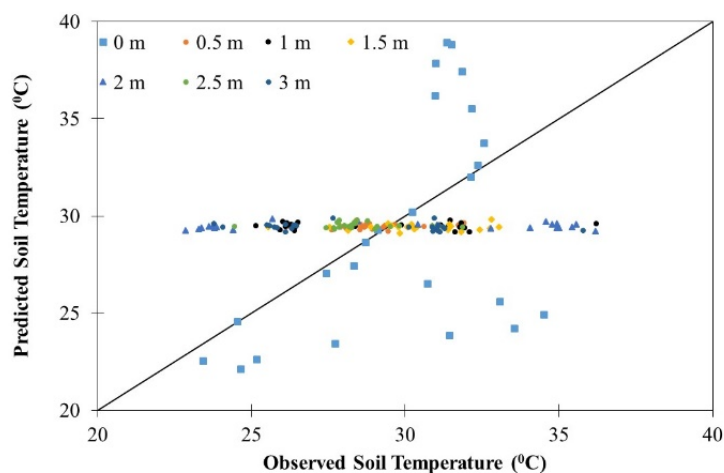


Figure 26 Comparison of predicted and observed soil temperature at various depths.

Conclusions

The 3-D numerical modeling of heat transport phenomenon in soil due to the change of sensible and latent heat under the ambient conditions of southern Thailand were presented in this paper. The effect of density, thermal conductivity, emissivity and absorptivity of soil, and latent heat on amplitude of soil temperature variation were investigated. Numerical results were validated by comparing them to the experimental results. It is concluded that the 3-D numerical model could predict the soil temperature to almost the same degree as results obtained by experimentation, especially at a depth of 1 m. The RMSE was in the range of 0.097 - 0.169. Finally, it was found that the variation of soil temperature occurred within 0.75 m only.

Acknowledgements

The authors would like to thank Thaksin University for funding this research project. Official thanks are given to the Thai Meteorological Department for providing the meteorological data. The authors also thank the Solar and Wind Energy Research Laboratory for their kind support of the experimentation.

References

- [1] G Mihalakakou, M Santamouris and D Asimakoupoulos. Modeling the thermal performance of earth to air heat exchangers. *Solar Energ.* 1994; **53**, 301-7.
- [2] M Santamouris, G Mihalakakou, C Balaras, A Argiriou and D Asimakoupoulos. Use of buried pipes for energy conservation in cooling of agricultural greenhouse. *Solar Energ.* 1995; **55**, 111-24.
- [3] NH Abu-Hamdeh. Measurement of the thermal conductivity of Sandy Loam and Clay Loam soils using single and dual probes. *J. Agri. Energ. Res.* 2001; **80**, 209-16.
- [4] OC Popiel, J Wojtkowiak and B Biernacka. Measurements of temperature distribution in ground. *Exp. Therm. Fluid Sci.* 2001; **25**, 301-9.
- [5] E Penrod, MJ Elliot and WK Brown. Soil temperature variation at Lexington, Kentucky. *J. Soil Sci.* 1960; **90**, 275-83.
- [6] JE Carson. Analysis of soil and air temperature by Fourier techniques. *J. Geophys. Res.* 1963; **68**, 2217-32.
- [7] G Mihalakakou. On estimating soil surface temperature profiles. *Energ. Build.* 2002; **34**, 251-9.
- [8] B Givoni and L Katz. Earth temperatures and underground buildings. *Energ. Build.* 1985; **8**, 15-25.

- [9] S Krishnaiah and DN Singh. A methodology to determine soil moisture movement due to thermal gradients. *Exp. Therm. Fluid Sci.* 2003; **27**, 715-21.
- [10] MMS El-Din. On the heat flow into the ground. *Renew. Energ.* 1999; **18**, 473-90.
- [11] G Mihalakakou, M Santamouris and D Asimakoupoulos. Modeling the earth temperature using multiyear measurements. *Energ. Build.* 1992; **9**, 1-9.
- [12] P Bloomfield. *Fourier Analysis of Time Series: An Introduction*. John Wiley & Sons, New York, USA, 1976.
- [13] CP Jacovides, G Mihalakakou, M Santamouris and JO Lewis. On the ground temperature profile for passive cooling applications in buildings. *Solar Energ.* 1996; **57**, 167-75.
- [14] JP Holman. *Heat Transfer*. John Wiley & Sons, New York, USA, 1997, p. 1-345.
- [15] J Hirunlabh, J Santisirisomboon and P Namprakai. Assessment of solar radiation for Thailand. *In: Proceedings of the International Workshop: Calculation Methods for Solar Energy System*, Université de Perpignan, France, 1994, p. 1-14.
- [16] P Namprakai and J Hirunlabh. A study of hourly to daily radiation ratio correlations at Bangkok, Thailand. *KMITT Res. Dev. J.* 1989; **12**, 40-51.
- [17] F Lasnier and WY Juen. The sizing of stand-alone photovoltaic systems using the simulation technique, RERIC. *Int. Energ. J.* 1990; **12**, 22-3.
- [18] B Givoni. Review and evaluation of cooling by long-wave radiation. *Passive Solar J.* 1982; **1**, 131-50.
- [19] J Waewsak, J Khedari, J Hirunlabh and R Sarachitti. The Study of Sky Emissivity in Thailand. *In: Proceedings of the 15th Mechanical Engineering Network*, Bangkok, Thailand, 2001, p. 32-6.
- [20] J Waewsak, J Khedari, R Sarachitti and J Hirunlabh. Direction and velocity of surface wind in Bangkok. *Thammasat Int. J. Sci. Tech.* 2002; **7**, 56-61.
- [21] N Klompong. 2008, The Study of Mathematical Modeling of Heat Transfer in Soil. Master Thesis, Thaksin University, p. 1-102.